Molecular Cancer Therapeutics

Spectrum and Degree of CDK Drug Interactions Predicts Clinical Performance

Ping Chen[1], Nathan V. Lee[2], Wenyue Hu[3], Meirong Xu[2], Rose Ann Ferre[1], Hieu Lam[2], Simon Bergqvist[2], James Solowiej[2], Wade Diehl[1], You-Ai He[1], Xiu Yu[1], Asako Nagata[1], Todd VanArsdale[2], and Brion W. Murray[2]

Abstract

Therapeutically targeting aberrant intracellular kinase signaling is attractive from a biological perspective but drug development is often hindered by toxicities and inadequate efficacy. Predicting drug behaviors using cellular and animal models is confounded by redundant kinase activities, a lack of unique substrates, and cell-specific signaling networks. Cyclin-dependent kinase (CDK) drugs exemplify this phenomenon because they are reported to target common processes yet have distinct clinical activities. Tumor cell studies of ATP-competitive CDK drugs (dinaciclib, AG-024322, abemaciclib, palbociclib, ribociclib) indicate similar pharmacology while analyses in untransformed cells illuminates significant differences. To resolve this apparent disconnect, drug behaviors are described at the molecular level. Nonkinase binding studies and kinome interaction analysis (recombinant and endogenous kinases) reveal that proteins outside of the CDK family appear to have little role in dinaciclib/palbociclib/ribociclib pharmacology, may contribute for abemaciclib, and confounds AG-024322 analysis. CDK2 and CDK6 cocrystal structures with the drugs identify the molecular interactions responsible for potency and kinase selectivity. Efficient drug binding to the unique hinge architecture of CDKs enables selectivity toward most of the human kinome. Selectivity between CDK family members is achieved through interactions with nonconserved elements of the ATP-binding pocket. Integrating clinical drug exposures into the analysis predicts that both palbociclib and ribociclib are CDK4/6 inhibitors, abemaciclib inhibits CDK4/6/9, and dinaciclib is a broad-spectrum CDK inhibitor (CDK2/3/4/6/9). Understanding the molecular components of potency and selectivity also facilitates rational design of future generations of kinase-directed drugs.
Mol Cancer Ther; 15(10); 2273–81. ©2016 AACR.

Introduction

Serine/threonine protein kinases are a large family of proteins that have essential roles in both physiology and the disease state making them attractive but challenging drug targets (1). A prominent example is cyclin-dependent kinases-4 and -6 proteins (CDK4/6) which regulate the G_1 restriction cell–cycle checkpoint that guards genomic integrity by preventing chromosome duplication until the necessary proteins are assembled (2–4). The molecular mechanism underlying this function includes activation by D-type cyclin proteins (5) leading to phosphorylation of the serine/threonine residues of the retinoblastoma (pRb) protein and E2F protein-mediated transcription of cell-cycle genes (e.g., cyclins A and E) as well as transcription-independent functions (e.g., chromatin structure; refs. 2, 5, 6). Multiple generations of CDK drugs have been created that bind in the ATP-binding cleft of CDK enzymes (Fig. 1; refs. 4, 7–9). This approach has proven challenging because sufficient on-target potency, kinome selectivity (1), and appropriate CDK family selectivity must be incorporated in a single molecule. The first generation of CDK-directed drugs (flavopiridol, roscovitine, olomucine) were nonspecific, pan-CDK, cytotoxic drugs which entered clinical trials in the 1990s and were found to be ineffective. Second-generation CDK-directed drugs were designed to be more potent and selective (dinaciclib, AT7519, R547, SNS-032, BMS-387032, AZD5438, AG-024322; refs. 7, 8). Dinaciclib is reported to be a CDK1/2/5/9 inhibitor which was evaluated for treating breast cancer patients but toxicities hampered its utility (10). In a phase I study, 60% of the patients experienced severe adverse events (11) and in a subsequent phase II study the fraction increased to 74% (12). AG-024322 is reported to be a CDK-selective drug but was not clinically efficacious (13). A lesson learned from the first two generations of CDK drugs is that toxicities often limit their clinical utility. Possible mechanisms contributing to the observed toxicities have been proposed – lack of a clear understanding of the mechanism of action, nonspecificity of the drugs, and inappropriate CDK family selectivity (7). This ambiguity has stunted the discovery of effective medicines that target this critical tumor biology.

A third generation of CDK-directed drugs is reported to be selective CDK4/6 inhibitors which have had impressive clinical performance in breast cancer patients resulting in breakthrough therapy designations (abemaciclib, palbociclib) and an FDA approval (palbociclib; refs. 4, 9). Breast cancer is expected to be susceptible to CDK4/6 inhibition for a number of reasons—(i) many patients have an intact pRb checkpoint (14), (ii) ER^+ breast cancer is dysregulated by aberrant cyclin D_1 expression

[1]Oncology Medicinal Chemistry, Pfizer Worldwide Research and Development, San Diego, California. [2]Oncology Research Unit, Pfizer Worldwide Research and Development, San Diego, California. [3]Drug Safety, Pfizer Worldwide Research and Development, San Diego, California.

Note: Supplementary data for this article are available at Molecular Cancer Therapeutics Online (http://mct.aacrjournals.org/).

Corresponding Author: Brion W. Murray, Pfizer Worldwide Research and Development, 10770 Science Center Drive, San Diego, CA 92121. Phone: 858-622-6038; Fax: 858-526-4240; E-mail: brion.murray@pfizer.com

doi: 10.1158/1535-7163.MCT-16-0300

or amplification (5), and (iii) CDK4/6 inhibitors trigger cell-cycle arrest in pRb-competent cells but not in pRb-inactive cells (15, 16). Surprisingly, single-agent studies of palbociclib encompassing 70 unselected patients resulted in only a single partial clinical response (17, 18). The structurally related ribociclib has similar single-agent findings ($n = 70$, 1 partial response; ref. 19). Subsequent nonclinical studies revealed additional complexity of G_1 restriction checkpoint regulation. Cyclin D_1 is a transcriptional target of the estrogen receptor which can mediate endocrine drug resistance in ER^+ breast cancer through persistent expression (5, 20). Synergy between CDK4/6 selective inhibitors and ER antagonists in blocking proliferation of ER^+ breast cancer tumor cells is observed (21). This led to the clinical strategy of combining CDK4/6 drugs with estrogen antagonists which resulted in the positive clinical results (20, 22–24). While palbociclib and ribociclib are most effective in combination with an ER antagonist, abemaciclib has significant single-agent activity (9 partial responses, $n = 36$ HR^+ breast cancer patients; ref. 19). The impact on human physiology with the drugs is also different. Palbociclib has primarily bone marrow toxicities ($n = 83$, 65% neutropenia, 23% leukopenia, 7% anemia) with little gastrointestinal (GI) toxicities (7% combined diarrhea/vomiting/nausea, from FDA label) which is consistent with selective CDK4/6 inhibition (25, 26). In contrast, abemaciclib has pervasive GI toxicities ($n = 47$, 57% nausea, 40% vomiting, 68% diarrhea, 18% fatigue) as well as bone marrow toxicities (40% neutropenia, 32% thrombocytopenia, 28% leukopenia, 18% anemia; refs. 19, 27). Another difference is the tolerated dosing schedules. Palbociclib and ribociclib are dosed intermittently (3 weeks on, 1 week off) while abemaciclib can be dosed continuously. Taken together, the clinical profiles of the third-generation drugs (7, 19, 28, 29) suggest that they impact patient biology in unique ways.

To date, the breadth of CDK-directed drug interactions has been incompletely characterized hampering the interpretation of clinical findings and the rational design of the next-generation therapies (7). The current study explores the range of biology impacted by CDK-targeted drugs using suites of biochemical, cellular, and structural assessments. The nexus of these approaches yields a nonclinical description for the range of activities the CDK drugs that is consistent with clinical responses and facilitates the discovery of next-generation therapies for the expected drug resistance (30).

Materials and Methods

A detailed description of the material and methods can be found in the Supplementary Section.

Cell lines

Cell lines described in this work were obtained from ATCC. Cell cultures were expanded by serial passaging and stocks frozen after 3–5 passages.

Purification of cell-cycle proteins

CDK6/cyclin D_1 and CDK4/cyclinD_3 protein pairs were expressed in insect cells and purified as complexes. CDK1, CDK2, cyclinA_2, and cyclin E_1 were expressed separately in insect cells and purified. CDK9/cyclin T_1 and CDK7/cyclinH_1/Mat1 were expressed in insect cells concomitantly, lysed, and purified. CDK5/p25 were expressed separately in insect cells, lysed, mixed together, and purified. Active site titrations with ATP-competitive inhibitors revealed that the active sites were competent (31). The pRb (residues 792-928) was expressed in *E. coli* and purified.

CDK6/cyclin D_1 radiometric assay measure phosphorylation of Rb protein

CDK6/cyclin D_1 reactions were preincubated (12 minutes, 30°C), initiatied with 75 μmol/L ATP (1 μCi [γ-^{32}P]-ATP), and terminated after 20 minutes. Product was captured and washed on a 96-well filter plate, Microscint-20 added, and quantitated. K_i values were derived from a fit to the Morrison equation (32, 33).

Mobility shift assays

CDK6/cyclin D_1 reactions monitored phosphorylation of 3 μmol/L 5FAM-Dyrktide (5FAM-RRRFRPASPLRGPPK) using a mobility shift assay (34). Inhibitor K_i reactions (45 minutes) were initiated with 2 mmol/L ATP after a preincubation (12 minutes, 22°C). K_i values were derived from a fit to the Morrison equation (32, 33). CDK1/2/4/5/7/9 were tested similarly. Screening assays were performed by Carna Biosciences (34).

pRb phosphorylation assay in tumor cell lines

Drugs were tested in an 11-point, 1:3 serial dilutions. Plates were incubated (24 hours), cells lysed, lysates transferred to ELISA plates (phospho-Rb-Ser_{780} or phospho-Rb-$Ser_{807/S811}$ rabbit mAb coated), incubated overnight at 4°C, washed, detected, luminescent GLO substrate reagent added, and quantitated.

Breast cancer cell proliferation assays

MCF7 and T47D parental cell lines were seeded at 1,500 cells/well. Drugs were titrated in duplicate from 10 μmol/L to 0.61 nmol/L in a 4-fold dilution scheme. On day 8 after compound addition, CellTiter-Blue viability reagent was added and fluorescence measured.

Cytotoxicity assay in rat gastrointestinal cells

Rat small-intestine epithelial cells (IEC-6, passage 6–16) were plated in 96-well plates. The following day, growth media were removed and media were added (0.1% FBS and DMSO or CDK drugs). Cell viability was quantified with the CellTiter-Glo Luminescent Cell Viability Assay (Promega). Luminescence was quantified and IC_{50} values were determined.

Cytotoxicity assay in rat neonatal cardiomyocytes

Hearts excised from 3- to 5-day-old pups (Wistar-Han rats) were digested with 0.08% trypsin–EDTA. Resulting cardiomyocytes were plated in collagen-coated plates. After 24 hours, media were changed to serum-free DMEM with 25 mmol/L glucose and cultured. Cardiomyocytes were seeded into 96-well plates and treated with DMSO or CDK4/6 inhibitors. After 72 hours, cell viability was measured using CellTiter-Glo luminescent cell viability assay (Promega).

Cell proliferation and cytotoxicity assay in human bone marrow mononuclear cells or peripheral blood mononuclear cells

Human bone marrow mononuclear cells (hBMNC) were purchased from Lonza and cultured in the hematopoietic progenitor growth medium in the presence of cytokines. Human peripheral

blood mononuclear cells (hPBMC) were purchased from Lonza and cultured in RPMI media. The hPBMCs or hBMNCs were treated with DMSO or CDK4/6 inhibitors in a 3-fold serial dilution in triplicate. After 24 hours (hPBMCs) or 5 days (hBMNCs) of continuous exposure, cell viability was measured using the CellTiter-Glo luminescent cell viability assay kit (Promega).

CDK6 and pCDK2 crystallization

The CDK6/compound complex was set up in sitting drops, 1:1 (protein to well buffer) with well buffer containing: 0.1 mol/L MES pH 6.0, 70–80 mmol/L NH_4NO_3, 10%–15% polyethyleneglycol 3350, and then incubated at 13°C. The rod-like crystals belong to space group I4 with unit cell dimensions $a = b = 102.2$ and $c = 59.8$ with one molecule per asymmetric unit.

pCDK2/cyclin E1 (FL pCDK2, cyclin E1 residues 96–378, 12–15 mg/mL) was set up in sitting drops containing 1:1 protein to buffer [0.1 mol/L MES pH 6, 180 mmol/L $Mg(HCO_2)_2$, 8%–11% polyethylene glycol 20,000] and incubated at 13°C to create beveled rod-like crystals ($P4_12_12$ space group with unit cell dimensions $a = b = 100.3$ and $c = 151.8$). Which were transferred to buffer supplemented with 1% DMSO and 0.5 mmol/L dinaciclib, incubated (12 hours, 13°C).

CDK6 and pCDK2 crystallography data collection and structure determination

Diffraction data were collected using a Pilatus 6M detector on beamline 17-ID and processed with auto-PROC (35). pCDK2/cyclinE/dinaciclib structure was determined using coordinates of 1W98 (36) protein. Refinement was carried out using autoBUSTER (37) at 2.8Å resolution. The initial CDK6/palbociclib complex structure was determined using coordinates of 3NUX (38). The CDK6/palbociclib structure was refined at 2.75Å using autoBUSTER. The CDK6/abemaciclib and CDK6/ribociclib complexes were refined using autoBUSTER at 2.27Å and 2.37Å, respectively. The data are summarized (Supplementary Table S1) and coordinates deposited into the PDB (5L2S, abemaciclib; 5L2W, dinaciclib; 5L2I, palbociclib; 5L2T, ribociclib).

Results

Cellular assessment of CDK drug behaviors

Key measures of drug performance are biochemical potency (IC_{50}), drug affinity (K_i, K_d), cellular potency (IC_{50}), and clinical drug exposure. As cellular analyses are commonly thought to be more predictive of clinical performance than biochemical analysis, on-target potencies of CDK-directed drugs were characterized in ER^+ breast cancer cell lines using both pharmacodynamic (phospho-pRb) and functional (proliferation) assessments. The pRb phosphorylation sites monitored are known to be phosphorylated by CDK4/6 ($Ser_{807/811}$, Ser_{780}; refs. 39, 40). Palbociclib and abemaciclib potently inhibit pRb phosphorylation (Ser_{780}, Ser_{807}) while ribociclib is less potent (Table 1). Interestingly dinaciclib is reported to be a CDK1/2/5/9 inhibitor (10, 41) but has similar pharmacodynamic potencies as the third-generation drugs. Using a functional endpoint, the third-generation drugs have similar potencies. Dinaciclib has potent antiproliferative activity but not strikingly more than abemaciclib and palbociclib (Table 1). AG-024322 is similarly potent to the other drugs but found to have low kinome selectivity so the data are separated (Supplementary Table S2). Taken together, tumor cell line studies find only modest differences for CDK-directed drugs.

To assess a wider range of biological functions of the CDK-directed drugs, their impact on normal cells was investigated. These contexts are critical to clinical drug performance because drug toleration defines the upper limit of clinical exposure possible. Cellular models of physiology are routinely used to characterize potential safety liabilities in the drug discovery process. In vitro models of the hematologic system (human bone marrow cells, peripheral blood mononuclear cells), gastrointestinal system (rat IEC-6 cells), and the heart (rat cardiomyocytes) are

Table 1. Biochemical and cellular potencies of selective CDK drugs

Analysis	Abemaciclib LY2835219	Palbociclib PD-0332991	Ribociclib LEE011	Dinaciclib SCH-727965
Biochemical				
CDK1/cyclinA_2 K_i (nmol/L)	330 ± 90	>1,400	>1,400	18 ± 3
CDK2/cyclinE_1 K_i (nmol/L)	150 ± 60	>2,500	>2,500	1.0 ± 0.3
CDK4/cyclinD_3 K_i (nmol/L)	0.07 ± 0.01	0.26 ± 0.03	0.53 ± 0.08	4.6 ± 0.6
CDK5/p35 K_i (nmol/L)	86 ± 12	>2,000	>2,000	0.85 ± 0.09
CDK6/cyclinD_1 K_i (nmol/L)	0.52 ± 0.17	0.26 ± 0.07	2.3 ± 0.3	1.7 ± 0.2
CDK7/cyclinH/MAT1 K_i (nmol/L)	220 ± 10	>2,000	>2,000	21 ± 2
CDK9/cyclinT_1 K_i (nmol/L)	4.1 ± 1.3	150 ± 10	190 ± 20	0.13 ± 0.04
PD in cells				
MCF7 IC_{50} (nmol/L)				
pRb-Ser_{807}	13 ± 4	20 ± 7.5	89 ± 36	5.6 ± 0.8
pRb-Ser_{780}	6.1 ± 1.4	9.3 ± 1.5	31 ± 8.2	4.3 ± 0.2
T47D IC_{50} (nmol/L)				
pRb-Ser_{807}	10 ± 2.9	21 ± 3.3	73 ± 18	10 ± 2.4
pRb-Ser_{780}	8.9 ± 5.9	17 ± 10	51 ± 30	11 ± 10
Cell proliferation				
Breast cancer (MCF-7) IC_{50} (nmol/L)	86 ± 14	120 ± 60	200 ± 90	8.7 ± 2.1
Breast cancer (T47D) IC_{50} (nmol/L)	94 ± 41	130 ± 80	260 ± 130	13 ± 1
Bone marrow mononuclear cells IC_{50} (nmol/L)	230 ± 27	240 ± 43	1,700 ± 231	9 ± 1.3
Cytotoxicity				
Peripheral blood mononuclear cells IC_{50} (nmol/L)	4,700 ± 175	18,000 ± 521	>10,000	11 ± 4.3
Intestinal epithelial crypt cells (rat) IC_{50} (nmol/L)	930 ± 187	4,700 ± 582	>10,000	<32
Cardiomyocytes (rat) IC_{50} (nmol/L)	7,200 ± 420	13,000 ± 672	6,000 ± 594	11 ± 3.5

NOTE: Biochemical potency is defined as binding affinities (K_i). Phosphorylation of pRb was monitored in two ER^+ tumor cell lines to measure pharmacodynamic effects. Surrogate cells from normal tissues were used to assess effects to normal physiology. All values are from at least three independent experiments.

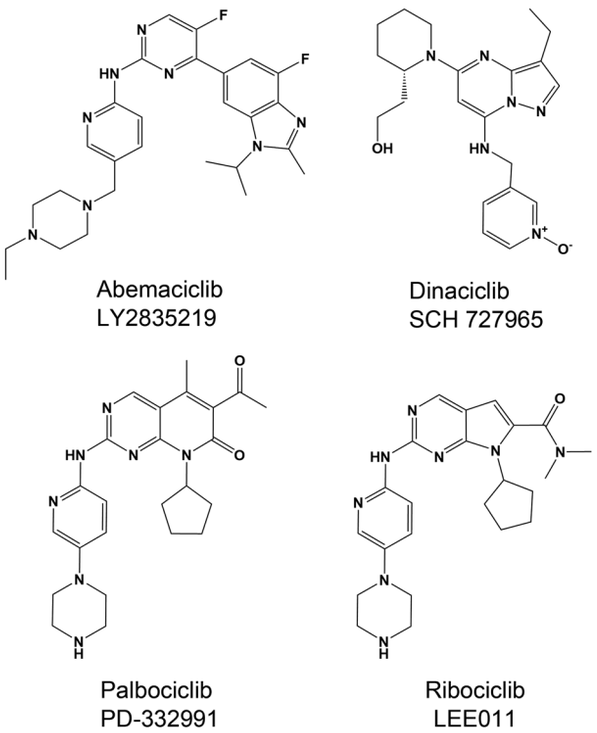

Figure 1.
Chemical structures of CDK4/6 selective drugs (abemaciclib, palbociclib, ribociclib) and the pan-CDK drug dinaciclib.

used to characterize effects on human physiology (Table 1). Third-generation drugs are more potent toward the proliferating bone marrow cells relative to the quiescent peripheral blood mononuclear cells. For bone marrow cells, palbociclib and abemaciclib have similar potency (IC_{50} = 220–240 nmol/L) while ribociclib is less potent (IC_{50} = 1,700 nmol/L). In GI cells, there are a range of activities for the three drugs (IC_{50} = 900 to >10,000 nmol/L) with abemaciclib having the most GI potency (IC_{50} = 900 nmol/L). The third-generation drugs have little effect on the terminally differentiated cardiomyocytes. Dinaciclib's profile in the normal cell models is distinct from the third-generation drugs because it is extremely potent (IC_{50} < 32 nmol/L) in all cellular assessments of physiology, reflecting a more cytotoxic profile. Taken together, drug performance in normal cells identifies key pharmacologic differences but not the molecular underpinnings.

Biochemical interaction analyses

Elucidation of the molecular processes affected by CDK drugs began by characterizing the breadth of their biophysical interactions with human proteins. Toward 17 functional proteins selected as sentinels for identifying nonkinase activities, there are no potent inhibitory activities detected for the drugs (Supplementary Table S3). Subsequent drug interaction analysis focused on the targeted enzyme family. Kinome selectivity was assessed with a panel of 274 human protein kinases (Supplementary Tables S4 and S5). Overall kinase selectivity is quantified by the kinase partition index (KPI) which meters selectivity relative to on-target potency (1 is perfectly selective, 0 is absolutely nonselective; refs. 42, 43). The drugs have a wide range of kinome selectivity profiles. AG-024322 has low kinase selectivity making it less useful for understanding CDK-driven biology (Supplementary Table S4). With CDK2 potency as the index activity, dinaciclib is not selective (KPI =0.21). Using the CDK most potently inhibited, the calculated kinase partition indices for the third-generation drugs are as follows: abemaciclib KPI = 0.88, palbociclib KPI = 0.96, ribociclib KPI = 0.99. Kinase inhibition data (relative to on-target potency) is mapped by kinase similarity (kinome tree analysis) to better understand the individual contributions to overall selectivity (Fig. 2). This analysis reveals that dinaciclib is extremely selective for the CDK protein family over the rest of the kinome (KPI = 0.98). Palbociclib and ribociclib molecules are highly selective for CDK4/6 relative to other human protein kinases. Abemaciclib has additional kinase activities (27 human protein kinases have K_i <50 nmol/L). Abemaciclib is a potent inhibitor (K_i < 10 nmol/L) of the DYRK, PIM, HIPK, and CaMK kinase families (Supplementary Table S5).

Target engagement analysis with an irreversible ATP probe is used to study drug interactions toward endogenous human kinases in an array of human tumor cell lines (PC3, THP1, Colo205, MCF7; Supplementary Table S6; ref. 44). The kinome selectivity analysis in PC3 and THP1 cells (selected for maximal kinome coverage) reveals that palbociclib and ribociclib are exquisitely selective for CDK4/6, and abemaciclib may have more complex pharmacology which includes potent CDK9 inhibition (e.g., GSK3, MPSK1, CaMK, CDK16/17/18; Supplementary Table S6A). Screening palbociclib in the clinically relevant tumor cell MCF7 (Supplementary Table S6B) shows potent CDK4 inhibition

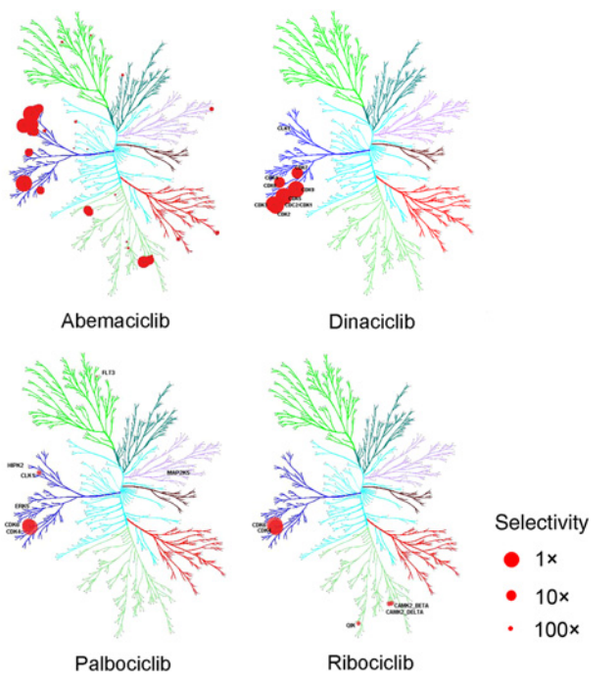

Figure 2.
Kinome selectivity of selective CDK4/6 inhibitors. The size of the circles represents the affinity of the drug for a particular protein relative to on-target potency; the bigger the circle, the higher the affinity. The on-target activity was either CDK4 (abemaciclib, palbociclib, ribociclib) or CDK2 (dinaciclib). Individual potency values are in Supplementary Table S5.

with a small number of other kinases affected. Dose–response analysis of palbociclib in a cell line that both CDK4 and CDK6 can be detected is used to benchmark screening values (Supplementary Table S6C). The IC_{50} values toward CDK4/6 are potent (40–140 nmol/L). The only other potently inhibited kinase is MPSK1/STK16 which is potently inhibited by abemaciclib and therefore unlikely responsible for the differential clinical behaviors. Taken together, the evaluation of kinome interactions reveals unique patterns of kinase modulation for each drug.

CDK family selectivity analysis

CDK family interaction analysis began by assessing the drugs in commercial screening assays which use affinity tagged proteins and do not account for time-dependent inhibition or tight-binding kinetics. This coarse analysis for the third-generation CDK drugs confirms the expected activities (CDK4, CDK6) and identifies possible additional activities for abemaciclib (CDK2, CDK9; Supplementary Table S7). Analysis of dinaciclib reveals broad CDK family interactions with CDK1/2/3/4/7/9 are potently inhibited (IC_{50} < 10 nmol/L). Because the predictability of biochemical results from CDK assays can be suboptimal for many reasons (e.g., protein construct design, purification methodology, post-translational modifications, assay format), a suite of assays was created on the basis of untagged, highly-purified, highly-active CDK enzymes which incorporated appropriate kinetic analysis to define the energetics of binding (K_i values; Table 1). The microfluidic electrophoretic mobility-shift biochemical assay (34) was benchmarked with the classic CDK biochemical analysis–[^{32}P]-phosphate incorporation into a pRb protein. Time-dependent inhibition of CDK6/cyclin D_1 is observed for palbociclib which is maximized with a 10-minute preincubation with CDK6/cyclin D_1. Incorporating time dependence and tight-binding constraints, palbociclib is determined to have potent affinity for CDK6/cyclin D_1 (K_i = 0.61 ± 0.04 nmol/L, n = 9). In the mobility shift assay, palbociclib potency toward CDK6/cyclin D_1 is very similar (K_i = 0.26 ± 0.07 nmol/L, n = 13; Table 1). Having benchmarked the mobility-shift assay format, it was used for detailed CDK-family selectivity analyses. The third-generation drugs are primarily CDK4 and CDK6 inhibitors yet they have distinct differences. Palbociclib has equivalent CDK4/cyclin D_3 and CDK6/cyclin D_1 potency while both ribociclib and abemaciclib are significantly more potent toward CDK4/cyclin D_3 (ribociclib is 5-fold, abemaciclib is 9-fold; Table 1). Toward CDK9/cyclin T_1, the third-generation drugs have measurable affinity but only abemaciclib achieves potent affinity (K_i = 4.1 ± 1.3 nmol/L). In contrast, dinaciclib has multiple CDK-inhibitory activities—CDK5/9 K_i <1 nmol/L, CDK2/4/6 K_i 1–5 nmol/L, and CDK1/7 K_i ∼ 20 nmol/L. AG-024322 also has a broad spectrum of CDK activities (Supplementary Table S2). The CDK interaction analyses reveal unique drug profiles that are expected to affect clinical pharmacology.

Analysis of clinical drug exposure data

To assess the translation of preclinical findings to clinical effects, a basic understanding of human exposure profiles of the drugs needs to be incorporated into the analysis. The dosing regimens and pharmacokinetics characteristics of the CDK drugs define the concentrations achieved and the duration of exposure (Supplementary Table S8). The exact nature of drug exposure is complex so a more general approach is used to achieve estimates of drug concentrations in different compartments of humans. Using human steady-state plasma drug concentrations (AUC_{0-24}) total and unbound (free) drug exposures can be calculated (Supplementary Table S8). This analysis indicates that palbociclib and ribociclib have CDK9 biochemical potencies that are unlikely to translate to systemic effects dependent on plasma drug distribution. Using the unbound (i.e., available for binding) abemaciclib drug concentration achieved in the clinic (C_{ave} = 35 nmol/L, C_{max} = 46 nmol/L; Supplementary Table S8) and the CDK9 K_i value (K_i = 4.1 nmol/L), CDK9 may contribute to clinical pharmacology. Dinaciclib has more pervasive CDK-family engagement (CDK2/3/4/5/6/9).

For oral therapies, the drug concentration in the gastrointestinal tract is substantially higher than in the plasma with the upper limit of unbound and total drug in the GI [35, 400 μmol/L (abemaciclib); 40, 280 μmol/L (palbociclib); and 410, 1,400 μmol/L (ribociclib); see Supplementary Methods]. Actual concentrations achieved in the clinic will be defined by many factors (e.g., patient-specific GI volume, dissolution rate, flux, fed state, solubility) but acknowledging that the GI drug concentration is substantially higher than the plasma exposure is useful to begin to evaluate drug-specific GI pharmacology. Evaluating drug affinities in vitro at permissive ATP concentrations (i.e., $K_{m,ATP}$) may overstate contributions (Supplementary Table S5A) so the inhibition can be calculated at more realistic concentration of the competitive ligand (1 mmol/L ATP) and expected drug concentrations (e.g., 10 μmol/L). This analysis reduces the list of potential off-target kinase activities expected to contribute to GI toxicities (Supplementary Table S5B). Taken together, the potential for polypharmacology is relative to both on-target potency and drug exposure achieved in the clinic.

Structural characterization of drug interactions with CDK2 and CDK6

Structural analyses of CDK-directed drug binding are conducted to identify molecular interactions that lead to the observed pharmacology. A CDK2–dinaciclib structure was reported in which dinaciclib binds to the inactive conformation of CDK2 (41). To profile the interaction of dinaciclib with the active, phosphorylated (pCDK2) conformation, the structure of dinaciclib/pCDK2/cyclin E was determined (Fig. 3). pCDK2 in this complex adopts the active configuration, characterized by the αC-helix orientation and the correct positioning of the activation loop. The salt bridge between catalytic residues

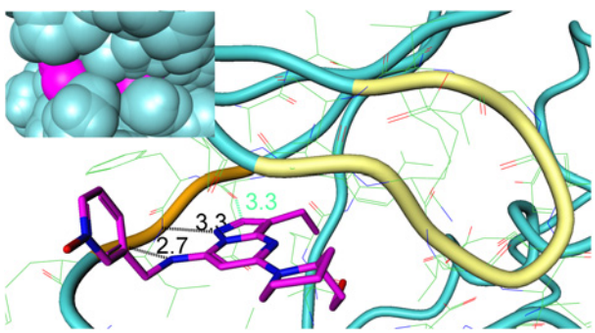

Figure 3.
Binding mode for dinaciclib. Crystal structure of pCDK2/cyclin E with dinaciclib (PDB 5L2W). The G-loop is colored in yellow and the hinge region in orange. Inserted figure represents the surfaces for pCDK2 in blue and dinaciclib in purple.

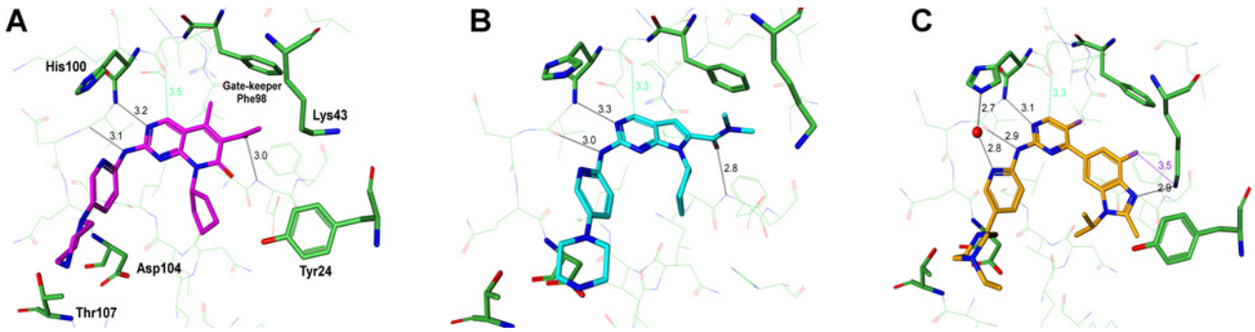

Figure 4.
Binding modes for third-generation drugs. CDK6 cocrystal structures for: palbociclib (**A**), ribociclib (**B**), and abemaciclib (**C**), with the binding site in a common orientation (PDB 5L2S, abemaciclib; 5L2I, palbociclib; 5L2T, ribociclib). Hydrogen bonds are rendered as dotted lines, and key active site residues are labeled.

Glu_{51} and Lys_{33} is another hallmark of this kinase active state. The bound conformation of dinaciclib is very similar to that in the CDK2 complex lacking cyclin E. The rms deviation between the two bound ligands on all nonhydrogen atoms is 0.36 Å. In this structure, the only direct protein-ligand hydrogen bonds are at the hinge region, between residues 81 and 83 and the drug's amino-pyrazolopyrimidine moiety. Dinaciclib binding is achieved predominantly through hydrophobic and van der Waals interactions. The catalytic cleft G-loop is well-ordered and adopts a closed conformation, making the ATP site more compact and enclosing dinaciclib within the ATP binding pocket (Fig. 3). This is further described by solvent-accessible surfaces that become buried upon ligand binding. In the complex, the buried surfaces for dinaciclib and pCDK2 are 377 $Å^2$ and 485 $Å^2$, respectively. As the total dinaciclib surface area is only 392 $Å^2$, most of the ligand (96%) is excluded from solvent. Additional selectivity over non-CDK family members comes from sequence differences at the hinge region. In most kinases, there is an additional glycine residue between residues corresponding to CDK2 His_{84} and Gln_{85}, which forces the polypeptide to bulge into the ATP site and clash with the dinaciclib binding mode. In summary, the shape complementarity of dinaciclib in pCDK2′s ATP binding pocket, along with the unique hinge sequence of CDK2, provide a structural rationale for the high potency and selectivity of dinaciclib toward CDK2 and similar CDKs.

The X-ray cocrystal structures of CDK6 and three third-generation drugs are determined in the absence of a cyclin D protein to define the spectrum of drug interactions at the atomic level (Fig. 4). In all three cases, CDK6 adopts a typical bi-lobal protein kinase fold that exhibits the inactive conformation; the αC-helix of the N-terminal lobe is displaced from the active site cleft, and the activation loop, though largely disordered, suggests an inactive configuration. The major differences between CDK6 active and inactive conformations occur in regions that do not directly contact the third-generation drugs. Drug binding to the inactive state is also characterized by isothermal calorimetry (Supplementary Table S9) to show that the rank ordering of the K_d values is the same as K_i values derived from enzymatic studies of active CDK6 (Table 1). The G-loop is mostly ordered in all three structures, with well-defined side chain density for Tyr_{24} (near the turn) in the complexes with palbociclib and abemaciclib, but less so with ribociclib. Each drug interacts with the hinge region using the same 2-aminopyrimidine group. In addition, there are several interactions unique to CDK6. The cocrystal structures reveal that the positively-charged piperazine ring of each drug is stabilized by lying against a solvent-exposed ridge consisting of Asp_{104} and Thr_{107}. In CDK1/2/3/5, the residue analogous to CDK6-Thr_{107} is lysine, which should cause electrostatic repulsion with the piperazine and thereby lower CDK1/2/3/5 potency. Interestingly, in CDK9, the corresponding residue is glycine, consistent with the measurable affinity of all three inhibitors for this family member. Finally, in the complex of CDK6-abemaciclib, an ordered water molecule is observed bridging the imidazole of hinge residue His_{100} and the ligand's pyridine nitrogen. Electron density for this water is not observed in the palbociclib and ribociclib complexes, possibly due to the resolution limit, nevertheless there is space for a water molecule at this position. Such a bridging interaction with His_{100} could contribute to favorable kinase selectivity, as this histidine residue is found in only 8 kinases based on sequence alignment (total of 442 kinases used for alignment). Within the CDK family, His_{100} is found only in CDK4/6. In another study, it was proposed that an inhibitor–His_{100} interaction might contribute to the observed 26-fold selectivity for CDK4/6 over other CDKs (38).

Despite the third-generation drugs achieving potent inhibition of CDK6, subtle yet critical differences in the binding interactions are observed. A hydrogen bond occurs between the invariant catalytic residue Lys_{43} and abemaciclib, which is not possible with the other drugs. Interactions with conserved catalytic residues would be expected to decrease kinase selectivity as they are common among kinases. Another difference in drug binding is that abemaciclib buries two fluorine atoms against the back wall of the ATP-binding pocket, whereas palbociclib and ribociclib present much larger substituents (ribociclib's dimethylamino group; palbociclib's methylketone and adjacent methyl) that might be more difficult to accommodate in other kinases. An intrinsic drug property that affects kinase selectivity for many inhibitors is lipophilicity, quantified by cLogP, which correlates with overall potency but not specificity (45, 46). The cLogP of abemaciclib (5.5) is significantly higher than palbociclib (2.7) or ribociclib (2.3), which allows abemaciclib to be more readily buried in the ATP cleft. Taken together, the structural studies reveal interactions common to the third-generation drugs but also differences that can impact their clinical behaviors.

Discussion

Cellular analyses are routinely used to characterize drug performance because isolated cells capture a subset of the biological complexity expected in the clinic (30). A limitation of this approach is that patients have a multitude of cellular environments with unique complements of expressed proteins that create a broad spectrum of signaling network architectures. As such, it is challenging to map clinical phenotypes of drugs to molecular processes using cell culture (30). For drugs that target intracellular signaling proteins (e.g., serine/threonine protein kinases), pharmacodynamic markers (e.g., pRb phosphorylation) can be modified by multiple enzymes obscuring the molecular mechanism of drug action. An alternative approach defines the array of biophysical interactions that a drug is capable of making which enables the connection to a wealth of known physiology. Previously, subsets of CDK drugs have been studied (41, 47–49) with more systematic comparisons occurring by literature reviews (4, 9, 19). In the current study, a synergistic combination of cellular, biochemical, and crystallographic analysis is used to characterize multiple generations of CDK drugs in a single study. This analysis began by assessing CDK drug interactions using a small panel of protein interaction sentinels that focused subsequent analyses on kinome selectivity. The second-generation CDK drugs encompass both ends of the selectivity spectrum. AG-024322 has low kinome selectivity and broad CDK family interactions which limits its utility to interrogate CDK biology while dinaciclib is exquisitely selective for a subset of the CDK kinase family. The cellular assessments of dinaciclib show equivalent potency for nontransformed cells and tumor cells. The third-generation drugs are selective kinase inhibitors but to differing degrees. As observed in both assessments using recombinant purified kinases and tumor cell target engagement approaches, the third-generation drug abemaciclib has more inhibitory activities outside the CDK family than dinaciclib yet has a superior selectivity for affecting tumor cells relative to untransformed cells. Palbociclib and ribociclib are extremely selective toward two CDKs (4/6) relative to the human kinome and the *in vitro* cellular models show that they are selectively effective for tumor cells. The analyses with endogenous kinases in tumor cells did not identify CDK9 interactions of palbociclib or ribociclib but did with abemaciclib (Supplementary Table S6). These findings are in-line with observed clinical responses—inhibiting CDK4/6 in patients produces effective, well-tolerated outcomes while more pervasive CDK family inhibition (e.g., dinaciclib) is less effective. Abemaciclib is shown to be different than palbociclib and ribociclib with more single-agent activity in the clinic so broader pharmacology should be expected. The kinome interaction assessments (purified proteins, tumor cell lysates) identify CDK9 as a likely candidate that contributes to abemaciclib's clinical pharmacology. It should be noted that another chemoproteomic study came to a different conclusion of about CDK9 selectivity but it used structural analogues of the CDK drugs to capture interacting kinases which could introduce kinase selectivity artifacts (47). Abemaciclib has significant biochemical potency for CDK5 so engagement of the atypical CDKs cannot be ruled out. In-line with this notion is the finding that abemaciclib potency inhibits CDK 16/18 in tumor cells (Supplementary Table S6A). As such, defining the exact nature of drug interactions with the CDK family is essential to understanding the molecular mechanisms of action. But kinase-inhibitory potencies alone are of limited value because they do not account for drug-specific clinical exposures.

The translation of CDK inhibitor activities to clinical effects is dependent on the human exposure profiles of the drugs because they define the degree and duration of target modulation (Table 1). This analysis indicates that palbociclib and ribociclib will only inhibit CDK4/6 while abemaciclib is expected to have an additional activity—CDK9. Previous biochemical analysis identified CDK9 as inhibited by abemaciclib but under-represented its CDK9 activity (IC_{50} = 57 nmol/L; ref. 7). Abemaciclib should cause a partial, steady-state inhibition of CDK9 (unbound exposure 7-fold greater than binding affinity) and intermittent, complete CDK9 inhibition (22-fold higher maximum unbound exposure relative to drug affinity). As such, abemaciclib is a CDK4/6/9 selective drug (Table 1). CDK9 is a critical enzyme that regulates a broad range of gene transcriptional events. The degree and timing of CDK9 inhibition is expected to cause clinically unique effects because these factors will define the subset of CDK9-dependent transcription events affected (50). Dinaciclib is reported to be a CDK1/2/5/9 drug based on previous findings (41). This analysis lacked the more predictive biochemical analyses as well as the incorporation of human exposure data. Dinaciclib is a more potent CDK9 inhibitor than abemaciclib which could translate to modulating a larger subset of CDK9-driven transcriptional events (50). Dinaciclib is also a more complete regulator of the G_1 restriction checkpoint because it potently inhibits CDK4/6 like the third-generation drugs but also inhibits CDK2 and CDK3. CDK3 is known to phosphorylate pRb ($Ser_{807/811}$) during the G_0–G_1 transition (51). In addition, the CDK2-inhibitory activity also affects other cell cycle checkpoint processes. Inhibition of the neurological kinase CDK5 by dinaciclib is not likely relevant because neurological toxicities do not present clinically. But since CDK5 is an atypical CDK related to CDK14 – 18 (52), it may a sentinel for additional CDK family activities for dinaciclib. Dinaciclib is a potent CDK1 inhibitor (K_i = 18 nmol/L) but since its unbound steady-state plasma concentration is 90 nmol/L (Table S8), this activity may not be clinically relevant. Therefore, dinaciclib should be considered a CDK2/3/4/6/9 drug. Dinaciclib illustrates that relevant kinase selectivity is not solely defined by the breadth of the affected kinome biology but the biological characteristics and the interconnectedness of the affected kinases. The third-generation drugs are oral therapies with a range of GI adverse event profiles. For oral therapies, the drug concentration in the GI is substantially higher than in the plasma. As the GI drug concentrations are high, the selectivity is evaluated at concentrations significantly higher than found in plasma (Supplementary Table S5B). From this analysis, palbociclib and ribociclib are expected to have minimal contributions from kinases outside of CDK4/6, while abemaciclib should completely inhibit CDK9 and may inhibit additional kinases (e.g., DYRK1B, HIPK2, PIM, CaMK2δ). Taken together, the observed clinical behaviors are consistent with the breadth and degree of CDK family engagement.

Protein–drug cocrystal structures expand our understanding of CDK inhibitor potency and kinome selectivity by identifying the underlying molecular interactions at an atomic level. In the previously determined co-crystal structure of palbociclib/

CDK6/v-cyclin, palbociclib binds to the active state of CDK6 (53). The study defines only interactions with a single conformation which is altered by a viral protein. A comprehensive, side-by-side analysis was undertaken on unactivated CDK proteins which enhances our understanding of the range of interactions that drugs can make. For example, dinaciclib achieves its potency and selectivity by targeting the ATP-binding pocket in a closed G-loop conformation with specific binding to the unique hinge sequence of the CDK family. However, these features do not provide selectivity within the CDK family. Cocrystal structures with third-generation drugs illuminate mechanisms for selective binding within the CDK family itself. Palbociclib and ribociclib molecules are highly selective for CDK4/6 relative to other CDKs as well as non-CDK kinases. Key elements of selectivity come from interactions with CDK4/6-specific residues such as His_{100} and Thr_{107} near the hinge region. Kinase specificity is enhanced when the drug molecules avoid interaction with highly conserved amino acids (like the catalytic lysine), or when they possess lower overall lipophilicity. Finally, the buried water configuration and ATP cavity topography are important features that fine-tune the selectivity of an inhibitor. Taken together, defining the molecular interactions of CDK drugs enables a better understanding of clinical responses and clinical utility. This knowledge provides a foundation for the rational design of future generations of CDK-directed drugs that will counter the expected drug resistance typically found with kinase-directed therapies (30).

Disclosure of Potential Conflicts of Interest

No potential conflicts of interest were disclosed.

Authors' Contributions

Conception and design: P. Chen, W. Hu, Y.-A. He, X. Yu, T. VanArsdale, B.W. Murray

Development of methodology: P. Chen, R.A. Ferre, J. Solowiej, Y.-A. He, T. VanArsdale, B.W. Murray

Acquisition of data (provided animals, acquired and managed patients, provided facilities, etc.): P. Chen, N. Lee, W. Hu, M. Xu, H. Lam, S. Bergqvist, J. Solowiej, W. Diehl

Analysis and interpretation of data (e.g., statistical analysis, biostatistics, computational analysis): P. Chen, N. Lee, W. Hu, H. Lam, S. Bergqvist, J. Solowiej, X. Yu, A. Nagata, T. VanArsdale, B.W. Murray

Writing, review, and/or revision of the manuscript: P. Chen, N. Lee, W. Hu, R.A. Ferre, S. Bergqvist, Y.-A. He, T. VanArsdale, B.W. Murray

Administrative, technical, or material support (i.e., reporting or organizing data, constructing databases): P. Chen, J. Solowiej, B.W. Murray

Study supervision: P. Chen, X. Yu, B.W. Murray

Acknowledgments

The authors thank Tae Sung for defining drug potency in untransformed cells and Tyzoon Nomanbhoy (ActivX Biosciences) for providing KiNativ profiling results.

Grant Support

Pfizer supported all of the studies.

Received May 12, 2016; revised July 21, 2016; accepted July 22, 2016; published OnlineFirst August 5, 2016.

References

1. Schwartz PA, Murray BW. Protein kinase biochemistry and drug discovery. Bioorg Chem 2011;39:192–210.
2. Talluri S, Dick FA. Regulation of transcription and chromatin structure by pRB: here, there and everywhere. Cell Cycle 2012;11:3189–98.
3. Santo L, Siu KT, Raje N. Targeting cyclin-dependent kinases and cell cycle progression in human cancers. Semin Oncol 2015;42:788–800.
4. Sherr CJ, Beach D, Shapiro GI. Targeting CDK4 and CDK6: From discovery to therapy. Cancer Discov 2016;6:353–67.
5. Witkiewicz AK, Knudsen ES. Retinoblastoma tumor suppressor pathway in breast cancer: prognosis, precision medicine, and therapeutic interventions. Breast Cancer Res 2014;16:207.
6. Zhu L. Tumour suppressor retinoblastoma protein Rb: a transcriptional regulator. Eur J Cancer 2005;41:2415–27.
7. Asghar U, Witkiewicz AK, Turner NC, Knudsen ES. The history and future of targeting cyclin-dependent kinases in cancer therapy. Nat Rev Drug Discov 2015;14:130–46.
8. Sanchez-Martinez C, Gelbert LM, Lallena MJ, de Dios A. Cyclin dependent kinase (CDK) inhibitors as anticancer drugs. Bioorg Med Chem Lett 2015;25:3420–35.
9. O'Leary B, Finn RS, Turner NC. Treating cancer with selective CDK4/6 inhibitors. Nat Rev Clin Oncol 2016;13:417–30.
10. Criscitiello C, Viale G, Esposito A, Curigliano G. Dinaciclib for the treatment of breast cancer. Expert Opin Investig Drugs 2014;23:1305–12.
11. Nemunaitis JJ, Small KA, Kirschmeier P, Zhang D, Zhu Y, Jou YM, et al. A first-in-human, phase 1, dose-escalation study of dinaciclib, a novel cyclin-dependent kinase inhibitor, administered weekly in subjects with advanced malignancies. J Transl Med 2013;11:259.
12. Mita MM, Joy AA, Mita A, Sankhala K, Jou YM, Zhang D, et al. Randomized phase II trial of the cyclin-dependent kinase inhibitor dinaciclib (MK-7965) versus capecitabine in patients with advanced breast cancer. Clin Breast Cancer 2014;14:169–76.
13. Brown AP, Courtney CL, Criswell KA, Holliman CL, Evering W, Jessen BA. Toxicity and toxicokinetics of the cyclin-dependent kinase inhibitor AG-024322 in cynomolgus monkeys following intravenous infusion. Cancer Chemother Pharmacol 2008;62:1091–101.
14. Ertel A, Dean JL, Rui H, Liu C, Witkiewicz AK, Knudsen KE, et al. RB-pathway disruption in breast cancer: differential association with disease subtypes, disease-specific prognosis and therapeutic response. Cell Cycle 2010;9:4153–63.
15. Dean JL, Thangavel C, McClendon AK, Reed CA, Knudsen ES. Therapeutic CDK4/6 inhibition in breast cancer: key mechanisms of response and failure. Oncogene 2010;29:4018–32.
16. Cadoo KA, Gucalp A, Traina TA. Palbociclib: an evidence-based review of its potential in the treatment of breast cancer. Breast Cancer 2014;6:123–33.
17. Flaherty KT, Lorusso PM, Demichele A, Abramson VG, Courtney R, Randolph SS, et al. Phase I, dose-escalation trial of the oral cyclin-dependent kinase 4/6 inhibitor PD 0332991, administered using a 21-day schedule in patients with advanced cancer. Clin Cancer Res 2012;18:568–76.
18. Schwartz GK, LoRusso PM, Dickson MA, Randolph SS, Shaik MN, Wilner KD, et al. Phase I study of PD 0332991, a cyclin-dependent kinase inhibitor, administered in 3-week cycles (Schedule 2/1). Br J Cancer 2011;104:1862–8.
19. Vidula N, Rugo HS. Cyclin-Dependent kinase 4/6 inhibitors for the treatment of breast cancer: a review of preclinical and clinical data. Clin Breast Cancer 2016;16:8–17.
20. Murphy CG, Dickler MN. The role of CDK4/6 inhibition in breast cancer. Oncologist 2015;20:483–90.
21. Finn RS, Dering J, Conklin D, Kalous O, Cohen DJ, Desai AJ, et al. PD 0332991, a selective cyclin D kinase 4/6 inhibitor, preferentially inhibits proliferation of luminal estrogen receptor-positive human breast cancer cell lines *in vitro*. Breast Cancer Res 2009;11:R77.
22. Dickson MA. Molecular pathways: CDK4 inhibitors for cancer therapy. Clin Cancer Res 2014;20:3379–83.
23. Migliaccio I, Di Leo A, Malorni L. Cyclin-dependent kinase 4/6 inhibitors in breast cancer therapy. Curr Opin Oncol 2014;26:568–75.

24. Finn RS, Crown JP, Lang I, Boer K, Bondarenko IM, Kulyk SO, et al. The cyclin-dependent kinase 4/6 inhibitor palbociclib in combination with letrozole versus letrozole alone as first-line treatment of oestrogen receptor-positive, HER2-negative, advanced breast cancer (PALOMA-1/TRIO-18): a randomised phase 2 study. Lancet Oncol 2015;16:25–35.
25. Laurenti E, Frelin C, Xie S, Ferrari R, Dunant CF, Zandi S, et al. CDK6 levels regulate quiescence exit in human hematopoietic stem cells. Cell Stem Cell 2015;16:302–13.
26. Scheicher R, Hoelbl-Kovacic A, Bellutti F, Tigan AS, Prchal-Murphy M, Heller G, et al. CDK6 as a key regulator of hematopoietic and leukemic stem cell activation. Blood 2015;125:90–101.
27. Morschhauser F, Bouabdallah K, Stilgenbauer S, Thieblemont C, Wolf M, de Guibert S, et al. Clinical activity of abemaciclib (LY2835219), a cell cycle inhibitor selective for CDK4 and CDK6, in patients with relapsed or refractory mantle cell lymphoma. Blood 2014;125:3067.
28. Vidula N, Rugo HS. Cyclin-dependent kinase 4/6 inhibitors for the treatment of breast cancer: a review of preclinical and clinical data. Clin Breast Cancer 2016;16:8–17.
29. Dukelow T, Kishan D, Khasraw M, Murphy CG. CDK4/6 inhibitors in breast cancer. Anti-cancer Drugs 2015;26:797–806.
30. Murray BW, Miller N. Durability of kinase-directed therapies-a network perspective on response and resistance. Mol Cancer Ther 2015;14: 1975–84.
31. Copeland RA. Evaluation of enzyme inhibitors in drug discovery. Hoboken, NJ: John Wiley & Sons, Inc.; 2005.
32. Morrison JF. Kinetics of the reversible inhibition of enzyme-catalysed reactions by tight-binding inhibitors. Biochim Biophys Acta 1969;185: 269–86.
33. Murphy DJ. Determination of accurate KI values for tight-binding enzyme inhibitors: an in silico study of experimental error and assay design. Anal Biochem 2004;327:61–7.
34. Perrin D, Fremaux C, Shutes A. Capillary microfluidic electrophoretic mobility shift assays: application to enzymatic assays in drug discovery. Expert Opin Drug Discov 2010;5:51–63.
35. Vonrhein C, Flensburg C, Keller P, Sharff A, Smart O, Paciorek W, et al. Data processing and analysis with the autoPROC toolbox. Acta Crystallogr D Biol Crystallogr 2011;67:293–302.
36. Honda R, Lowe ED, Dubinina E, Skamnaki V, Cook A, Brown NR, et al. The structure of cyclin E1/CDK2: implications for CDK2 activation and CDK2-independent roles. EMBO J 2005;24:452–63.
37. Smart OS, Womack TO, Flensburg C, Keller P, Paciorek W, Sharff A, et al. Exploiting structure similarity in refinement: automated NCS and target-structure restraints in BUSTER. Acta Crystallogr D Biol Crystallogr 2012; 68:368–80.
38. Cho YS, Borland M, Brain C, Chen CH, Cheng H, Chopra R, et al. 4-(Pyrazol-4-yl)-pyrimidines as selective inhibitors of cyclin-dependent kinase 4/6. J Med Chem 2010;53:7938–57.
39. Narasimha AM, Kaulich M, Shapiro GS, Choi YJ, Sicinski P, Dowdy SF. Cyclin D activates the Rb tumor suppressor by mono-phosphorylation. eLife. 2014:e02872.
40. Rubin SM. Deciphering the retinoblastoma protein phosphorylation code. Trends Biochem Sci 2013;38:12–9.
41. Parry D, Guzi T, Shanahan F, Davis N, Prabhavalkar D, Wiswell D, et al. Dinaciclib (SCH 727965), a novel and potent cyclin-dependent kinase inhibitor. Mol Cancer Ther 2010;9:2344–53.
42. Cheng AC, Eksterowicz J, Geuns-Meyer S, Sun Y. Analysis of kinase inhibitor selectivity using a thermodynamics-based partition index. J Med Chem 2010;53:4502–10.
43. McTigue M, Murray BW, Chen JH, Deng YL, Solowiej J, Kania RS. Molecular conformations, interactions, and properties associated with drug efficiency and clinical performance among VEGFR TK inhibitors. Proc Natl Acad Sci U S A 2012;109:18281–9.
44. Patricelli MP, Nomanbhoy TK, Wu J, Brown H, Zhou D, Zhang J, et al. In situ kinase profiling reveals functionally relevant properties of native kinases. Chem Biol 2011;18:699–710.
45. Tarcsay A, Keseru GM. Contributions of molecular properties to drug promiscuity. J Med Chem 2013;56:1789–95.
46. Zhang C, Lopez MS, Dar AC, Ladow E, Finkbeiner S, Yun CH, et al. Structure-guided inhibitor design expands the scope of analog-sensitive kinase technology. ACS Chem Biol 2013;8:1931–8.
47. Sumi NJ, Kuenzi BM, Knezevic CE, Remsing Rix LL, Rix U. Chemoproteomics reveals novel protein and lipid kinase targets of clinical CDK4/6 inhibitors in lung cancer. ACS Chem Biol 2015;10:2680–6.
48. Gelbert LM, Cai S, Lin X, Sanchez-Martinez C, Del Prado M, Lallena MJ, et al. Preclinical characterization of the CDK4/6 inhibitor LY2835219: in-vivo cell cycle-dependent/independent anti-tumor activities alone/in combination with gemcitabine. Invest New Drugs 2014;32:825–37.
49. Toogood PL, Harvey PJ, Repine JT, Sheehan DJ, VanderWel SN, Zhou H, et al. Discovery of a potent and selective inhibitor of cyclin-dependent kinase 4/6. J Med Chem 2005;48:2388–406.
50. Garriga J, Grana X. CDK9 inhibition strategy defines distinct sets of target genes. BMC Res Notes 2014;7:301.
51. Ye X, Zhu C, Harper JW. A premature-termination mutation in the Mus musculus cyclin-dependent kinase 3 gene. Proc Natl Acad Sci U S A 2001; 98:1682–6.
52. Malumbres M.Cyclin-dependent kinases. Genome Biol 2014;15:122.
53. Lu H, Schulze-Gahmen U. Toward understanding the structural basis of cyclin-dependent kinase 6 specific inhibition. J Med Chem 2006;49: 3826–31.